Abdominal Radiology (2019) 44:2418–2429
https://doi.org/10.1007/s00261-019-01993-6

HEPATOBILIARY

Comparison of CT methods for determining graft steatosis in living donor liver transplantation

Mehmet Şeker[1] · Cengiz Erol[1] · Şinasi Sevmiş[2] · Burcu Saka[3] · Afak Durur Karakaya[1]

Published online: 1 April 2019

Abstract

Purpose To evaluate and compare the diagnostic performance of non-enhanced computed tomography (NECT) and contrast-enhanced CT (CECT) attenuation indices in the assessment of hepatic steatosis by using biopsy as the reference standard.

Materials and methods This retrospective study was approved by our Institutional Review Board. 55 Potential donors who underwent both NECT and triphasic CECT and core liver biopsy, were included the study. Average attenuation measurements that were obtained from multiple regions in liver, spleen, and psoas muscle on both unenhanced and CECT were used for analysis. Hepatic attenuation measurements were analyzed with and without normalization with the spleen and psoas muscle. Linear regression and receiver operating characteristic (ROC) curve analysis were used to evaluate the statistical association between CT indices and steatosis at histology.

Results Linear regression analysis confirmed the strongest correlation between steatosis and normalized measurements of hepatic attenuation with splenic attenuations on hepatic venous phase of CECT scan (R 0.821; R^2 0.674 and R 0.816; R^2 0.665, respectively). The use of ROC curve analysis also demonstrated that normalized measurements of hepatic attenuation with splenic attenuations on hepatic venous phase of CECT showed high diagnostic performance regarding the qualitative distinction of steatosis (AUC values greater than 0.9).

Conclusion Attenuation measurements of liver normalized with spleen on hepatic venous phase may be useful in evaluating steatosis in donor candidates with moderate to severe steatosis who are unacceptable for liver donation. In this manner unnecessary liver biopsy may be avoided in those donor candidates.

Keywords Hepatic steatosis · Living donor liver transplantation (LDLT) · Contrast-enhanced CT · Non-enhanced CT

Introduction

Living donor liver transplantation (LDLT) is being increasingly used as definitive therapeutic option in management of patients with end-stage liver disease due to limited availability of cadaveric donor organ donations. However, it is a complicated procedure and a healthy living donor is

This manuscript has not been published and is not under consideration for publication elsewhere. All authors have approved the manuscript and agree with its submission to Abdominal Radiology.

Electronic supplementary material The online version of this article (https://doi.org/10.1007/s00261-019-01993-6) contains supplementary material, which is available to authorized users.

✉ Mehmet Şeker
hikmet.irfan@hotmail.com

Cengiz Erol
drcengizerol@yahoo.com

Şinasi Sevmiş
sinasi.sevmis@gophastanesi.com.tr

Burcu Saka
burcusaka99@gmail.com

Afak Durur Karakaya
afakdurur@yahoo.com

[1] Department of Radiology, Faculty of Medicine, Medipol University, Bağcılar, 34214 Istanbul, Turkey

[2] Department of Surgery, Yeni Yuzyıl University, Gaziosmanpaşa, 34245 Istanbul, Turkey

[3] Department of Pathology, Faculty of Medicine, Medipol University, Bağcılar, 34214 Istanbul, Turkey

concomitantly placed at risk [1–3]. Donor evaluation is one of the most important aspects of LDLT. The evaluation process should reveal any conditions that may predispose the healthy donor to any intra and post-operative complications.

Hepatic steatosis is an important risk factor in liver surgery and the adverse effects of steatosis in liver surgery were at first acknowledged in transplantation studies. Hepatic steatosis is now known to adversely affect the outcome of hepatic transplantation [4–7]. Hepatic steatosis is the most common diffuse liver condition that may disqualify an otherwise healthy person from being a liver donor. Up to 30% of living liver donor candidates are rejected for presenting steatosis [8, 9].

In cases of cadaveric donor transplantation, the use of marginal donors has been discussed worldwide. But only perfect "or almost perfect" livers can be used in LDLT, as donor safety is the highest priority in LDLT [8, 10]. There are no consensus for the acceptable range of steatosis in LDLT, but it is generally accepted that moderate or severe (greater than 30%) steatosis should be avoided, to prevent complications in the donor [8, 11, 12]. However, the actual risk of mild steatosis in living liver donors remains to be elucidated [8]. Because of this some centers have the cut-off set at 10% for acceptability as a donor and some centers, like ours, consider 20% or more degree of steatosis as contraindication for donation [12–15].

Liver biopsy is the standard method for assessment of steatosis. In addition liver biopsy is also useful in excluding occult chronic liver disease. Liver biopsies, in an otherwise suitable donor with normal liver function test results, may discover abnormalities most of which were non-specific findings of unknown significance [15, 16]. But the role of liver biopsy in donor selection remains controversial, since the procedure carries potential risks for the donor candidate. Some transplantation centers advocate routine liver biopsy as part of donor evaluation and some perform liver biopsy on potential donors based on clinical and imaging findings that suggest some degree of concern regarding histological status of the liver [16]. Although liver biopsy is known to be a safe procedure, it is still an invasive procedure that may cause morbidity. Furthermore it is prone to sampling errors and the determination is semi-quantitative [17, 18]. In order to overcome these potential limitations of biopsy, various imaging techniques have been employed for the evaluation of steatosis in preoperative donor liver evaluation. However, there is no consensus as to which imaging modality should be used or regarding the threshold values that should be used to identify hepatic steatosis and to suggest which patients require biopsy [15].

Among cross-sectional imaging modalities, magnetic resonance imaging (MRI) is currently considered as being the most effective non-invasive method for the diagnosis of steatosis [3, 16, 19, 20]. The degree of steatosis can be determined by either using gradient-echo chemical shift imaging (Dixon method) or proton MR spectroscopy. Previous studies have demonstrated that MRI can be used to evaluate hepatic steatosis and can be used as an initial evaluation tool to determine the necessity of selective preoperative liver biopsy in LDLT [15, 21, 22].

The donor liver evaluation includes not only assessment of hepatic parenchyma but also assessment of the hepatic volume, vascular and biliary anatomy, and a multistep evaluation protocol is used. Multidetector computed tomography (CT) permits reasonable assessment of the hepatic parenchymal morphology in conjunction with estimation of the liver volumes and a detailed analysis of vascular anatomy. In many transplantation centers, to simplify and shorten time-consuming and costly procedures, CT has been most widely used as a comprehensive tool although it is considered to be less sensitive in the assesment of hepatic steatosis than MRI [1, 23].

Non-enhanced CT (NECT) has long been used to evaluate hepatic steatosis on the basis of the inverse relationship between the amount of steatosis and the hepatic attenuation at CT and it is generally assumed that NECT may provide a reasonable assessment of steatosis [17, 19, 21, 24, 25]. In some reports, researchers suggested that NECT might preclude liver biopsy in some of liver donor candidates who have an unacceptable degree of steatosis and may be used as a screening tool that would minimize unnecessary liver biopsy in patients with an unacceptable degree of hepatic steatosis for transplantation [21, 25]. But despite the widespread use, there is conflicting evidence to as to whether or not it can accurately quantitatively estimate steatosis [17, 24–28].

Whether these methods for diagnosing fatty infiltration of the liver can be applied to contrast-enhanced CT (CECT) is an important question. There have been studies [24, 26–28] regarding the diagnosis of steatosis on CECT and some of these [26, 27, 29] showed a high accuracy of CECT. But most of these studies [19, 24, 30] showed lower accuracy of CECT compared with NECT and suggested that contrast material related factors such as iodine concentration, volume and rate of injection, and scanning delays, influence the hepatic attenuation to varying degrees and may mask subtle differences in attenuation caused by steatosis. However most of the previous studies lacked pathological correlation and were not designed to allow a definitive comparison between CECT and NECT as NECT was used as the reference standard [27–30].

Another issue is that there are several attenuation indices that have been used to assess steatosis with CT. These include measurement of liver attenuation only and normalization of hepatic attenuation with splenic and muscle attenuation. But there is no consensus on which method is best for predicting hepatic steatosis [17, 21, 24–28, 31–33].

We thought that it will be valuable to understand the capability of CECT for the diagnosis of hepatic steatosis as it is used often without concomitant NECT. If diagnostic accuracy of CECT for diagnosing and quantification of steatosis is proved, CT protocols for preoperative donor evaluation may be reviewed with the purpose of avoiding unnecessary scan phases. Also we felt it necessary to reevaluate diagnostic accuracy of NECT as it is widely employed for diagnosing steatosis. In this study we used attenuation measurements of liver only and liver attenuation normalized with spleen and muscle attenuations on both NECT and CECT scans in order to evaluate and compare the diagnostic performance of CT indices in the assessment of hepatic steatosis by using biopsy as the reference standard.

Materials and methods

Study population

This study was approved by our Institutional Review Board. All subjects gave written informed consent for CT imaging.

We retrospectively reviewed the database of 134 donor candidates who were evaluated for LDLT at our institution between May 2014 and February 2017. Our liver transplantation center was performing US-guided liver biopsy on all potential donors unless there were any abnormal findings other than hepatic steatosis on CT that might preclude liver donation until December 2015. Later on a different donor evaluation protocol was adopted and liver biopsy was performed only on selected cases based on clinical and imaging findings. Out of these donor candidates, 55 potential donors who underwent both NECT and triphasic CECT and core liver biopsy were included the study. Donor candidates whom liver biopsy were not performed, were excluded from the study. The interval between preoperative CT and donor biopsy was not greater than 1 week.

In these 55 candidates, the mean age was 37.18 years, with a range of 21–60 years. These included 37 men (mean age 37.18 years; SD 7.93; range 21–58 years) and 18 women (mean age 42.22 years; SD 10.1; range 21–60 years).

CT imaging protocol

All CT scans were obtained with a 256 slice multidetector row CT scanner (Brilliance iCT, Philips Healthcare, Best, the Netherlands). NECT and CECT scanning were performed from the lung base through pelvic inlet. CECT imaging was performed following the dynamic injection of non-ionic low osmolar iodinated contrast material. For the CECT scans, all patients received a dose of 1.5 mL/kg body weight contrast material with a standard iodine concentration of 350 mg I/mL (iohexol 350 mg I/mL, Omnipaque, Opakim Medical Products, Inc., Istanbul, Turkey). The contrast material (warmed to body temperature) was administered intravenously by means of an automatic power injector (Medrad® Stellant® CT Injection System, Bayer HealthCare LLC, Pittsburg, USA) with a rate of 4 mL/s followed by 50 ml of saline solution at a flow rate of 4 mL/s through an 22 gauge angiographic catheter into an antecubital vein.

Arterial phase imaging was performed using a bolus tracking technique, i.e., 10 s delay after the aortic attenuation at the level of the diaphragm had reached 120 Hounsfield units (HU). Portal inflow (parenchymal) phase and hepatic venous (late venous) phase images were obtained approximately 55–60 s and 75–80 s after the initiation of intravenous contrast material administration respectively.

The technical parameters utilized at CT scans for NECT and CECT imaging were the following: slice collimation 128×0.625 mm, beam pitch 0.99, gantry rotation time 0.5 s, section thickness 1 mm, reconstruction interval 1 mm, voltage 120 kVp. CT scans were performed using an automated dose modulation system (Automatic DoseRight ACS, Philips Healthcare, USA) with the maximal allowable tube current set at 200 mA.

The data were transferred to workstation (Philips Intellispace Portal Workstation, Philips Healthcare, Best, The Netherlands) from picture archiving and communication System (Centricity Universal Viewer, GE Medical Systems, Milwaukee, WI, USA) for imaging post-processing and analysis and all the images were interpreted by a single observer with 10 year experience in imaging diagnosis.

Image analysis

Image analysis for hepatic steatosis was assessed by a radiologist blinded to histopathologic findings. We measured the HU of the liver, spleen, and psoas muscles by using region-of-interest (ROI) measurement of CT attenuation on NECT and CECT scans (Fig. 1).

Since all patients included in the study were right lobe LDLT donor candidates and liver biopsies were performed only from the right lobe of the liver, the CT attenuations of liver were measured only from right lobe. In addition, the attenuation of the right hepatic lobe was found to be lower than that of the left lobe because of the differential distribution of liver fat. In diffuse steatosis, particularly the non-cirrhotic type, there is a preferential distribution of steatosis toward the right hepatic lobe because of the physiologically greater portal flow to the right lobe than to the left lobe [19]. As our study is retrospective, we cannot warrant location-to-location correlation between the pathologic specimens and the attenuation measurements. In order to overcome this limitation we measured multiple ROIs from the right lobe and used the average value for analysis. The hepatic attenuation was measured by averaging the HU values of 8 circular

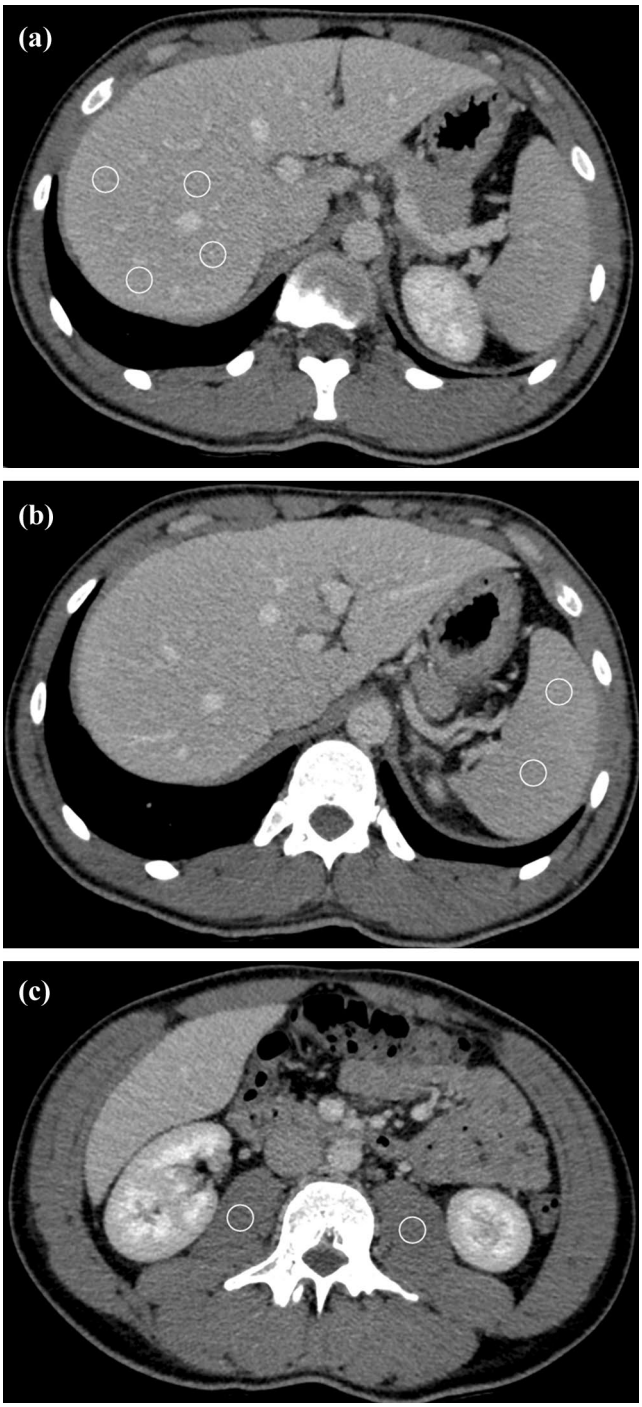

Fig. 1 Hepatic venous phase contrast-enhanced CT images of 35-year-old male donor candidate showing circular ROIs (100–105 mm^2) placed with care so as not to include macroscopic vessels. **a** Image shows 4 ROIs (white circles) placed at two different sites in segments 7 and 8 of the liver. **b** Image shows 2 ROIs (white circles) placed at middle third of the spleen. **c** Image shows 2 ROIs (white circles) placed one in left and one in right psoas muscle

ROI's (100–105 mm^2), that were placed at 2 different sites (central and peripheral portion) in each segment of the right hepatic lobe according to Courinaud's system. We tried to match the biopsy sites and the locations of the ROIs at CT as closely as possible. Care was taken to sample homogeneous areas representative of the parenchyma, with avoidance of vessels, bile ducts and focal lesions.

The splenic attenuation was obtained by averaging the 6 HU values at three different (the upper third, middle third, and lower third of the spleen) level. For each level 2 ROI's (100–105 mm^2) was placed with care so as not to include macroscopic vessels.

The psoas muscle attenuation measurements were obtained by averaging 2 HU values of one ROI in the left and one in the right.

For each candidate, five different CT indices were obtained by using both NECT and triphasic CECT images; liver attenuation only on non-enhanced, arterial, portal inflow, and hepatic venous phases (*L*, *A*, *P*, and *V*, respectively), difference between the hepatic and splenic attenuation on non-enhanced, arterial, portal inflow, and hepatic venous phases ($L - S$, $aL - S$, $pL - S$ and $vL - S$, respectively), liver to spleen attenuation ratio on non-enhanced, arterial, portal inflow, and hepatic venous phases (*L*/*S*, aL/*S*, pL/*S*, and vL/*S*, respectively), difference between the hepatic and psoas muscle attenuation on non-enhanced, arterial, portal inflow, and hepatic venous phases ($L - M$, $aL - M$, $pL - M$, and $vL - M$, respectively) and liver to psoas muscle attenuation ratio on non-enhanced, arterial, portal inflow, and hepatic venous phases (*L*/*M*, aL/*M*, pL/*M*, and vL/*M*, respectively).

Histologic analysis

US-guided liver biopsy was performed by a interventional radiologists with 18-gauge needles (Tru-Core™ II Automatic Biopsy Instrument; Argon Medical Devices, Dallas, USA). In all donor candidates, biopsy specimens were obtained from the right hepatic lobe by using an intercostal approach. Two biopsy specimens were obtained from every candidate. These sites were located approximately between hepatic segments V, VI, VII, and VIII.

A pathologist, who was blinded to the radiologic findings, evaluated the liver biopsy samples for histopathologic grading of hepatic steatosis. The slides for histological review were prepared with haematoxylin–eosin staining for evaluation of the degree of steatosis. The histological degree of steatosis was visually assessed using a percentage scale of the amount of liver parenchyma replaced by steatotic droplets. Because 1–4% hepatic steatosis is clinically non-significant, donor candidates who have steatosis less than 5% in biopsy specimens, were considered as non-steatotic and candidates who have steatosis equal to or greater than 5%

in specimens are considered as steatotic. For our study, the degree of steatosis at histologic analysis was used as the reference standard.

Data and statistical analysis

Statistical analyses were performed by using SPSS 16.0 for Windows (SPSS, Chicago, IL, USA). The statistical association between steatosis at histologic analysis and all CT indices was analyzed using the linear regression. A p value of less than 0.05 was considered significant. The standard error of the estimate between the degree of steatosis at histology and those estimated with the regression equations were calculated. Receiver operating characteristic (ROC) curve analysis was also carried out in order to evaluate which indices were best associated with the presence and severity of steatosis. The area under the ROC curves (AUC) and 95% confidence intervals (CIs) were calculated and compared among CT indices. A two-sided value of p value of less than 0.05 was considered significant. The cut-off values that provided a balance between sensitivity and specificity and the highest cut-off values that yielded 100% specificity were determined by using Youden Index.

Results

Histologic analysis

In the 55 donor candidates, the degree of steatosis at histologic analysis ranged from 0 to 30% (mean ± SD 10.31% ± 10.27). Of these, 24 potential donor livers (43.6%) were non-steatotic (mean ± SD 1.25% ± 1.51, range 0–3%) and remaining 31 potential donor livers (56.4%) had steatosis (mean ± SD 17.32% ± 8.48, range 5–30%) on histology. 16 Potential donor livers (29.1%) had equal to or greater than 20% (the cut-off set for acceptability as a donor in our center) steatosis (mean ± SD 24.69% ± 3.86, range 20–30%) on histology and were not accepted for LDLT. Remaining 39 donor candidates (70.9%) were accepted for LDLT (mean ± SD 4.41% ± 4.627, range 5–30%).

CT and histologic analysis

The attenuation values (mean ± SD and range) of liver, spleen and psoas muscle, the data for all CT indices (mean ± SD and range) are presented in Table 1.

With the changes in the degree of hepatic steatosis, there was no significant difference in splenic attenuation. But the SD of spleen CT attenuation in CECT scans was significantly higher than in NECT scans. This change in SD of spleen CT attenuation was more pronounced in arterial phase CT scans.

There was also marked difference in liver CT attenuation values in CECT scans, except arterial phase CT scan in non-steatotic liver. The change in SD of liver CT attenuation was higher in portal and hepatic venous phases. But these changes in SD of liver and spleen attenuations were almost equal in portal and hepatic venous phases.

There was no difference in the SD of psoas muscle CT attenuation when cathegorzed by the degree of hepatic steatosis. Furthermore there was no difference in the SD of psoas muscle CT attenuation in different phases of CECT scans.

Results of linear regression analysis

Linear regression analysis confirmed a very strong correlation between steatosis and vL − S and vL/S (R 0.821, R^2 0.674 and R 0.816, R^2 0.665, respectively). There was also a strong correlation between steatosis and pL − S and pL/S (R 0.739, R^2 0.546 and R 0.735, R^2 0.540, respectively). All NECT indices had lower but strong correlation with steatosis. But the difference among these was small.

The standard error of the estimate (S^2) between the degree of steatosis at histology and those estimated with the regression equations varied between 5.920 and 9.843.

The results of linear regression analysis for NECT and CECT scans are shown in Table 2.

Performance of CT in the diagnosis of presence and severity of steatosis

On the basis of the presence or absence of steatosis, vL/S, vL − S, L/M, L − M, pL/S, and pL − S were highly predictive with AUC of greater than 0.9. L, L − S, L/S, A, aL − M, aL/M, had AUC values greater than 0.8. There was no statistical difference between these AUC values (p values between 0.13 and 0.98).

vL − S and vL/S were also highly predictive in discriminating steatosis equal to or greater than 20% and steatosis less than 20%, with AUC values of 0.950 and 0.947 respectively. L, L/S, L − S, pL − S, and pL/S were also good predictors with high AUC values (ranging between 0.870 and 0.876). There was also no statistical difference between these AUC values (p values between 0.27 and 0.96).

The ROC curve analysis for the diagnosis of presence and absence of steatosis and of steatosis 20% or greater are shown in Table 3.

The cut-off values in the diagnosis of presence and severity of steatosis

The cut-off values that provided a balance between sensitivity and specificity for the diagnosis of presence and absence of steatosis were 2.5 for L − M and 1.04 for L/M and L − M and L/M had the highest overall accuracy rates (89%). But

Table 1 CT attenuation indices categorized according to hepatic steatosis

CT indices	Hepatic fat content (%)	Non-enhanced CT		Arterial phase CT		Portal inflow phase CT		Hepatic venous phase CT	
		Attenuation[a] (HU)	Range (HU)	Attenuation[a] (HU)	Range (HU)	Attenuation[a] (HU)	Range (HU)	Attenuation[a] (HU)	Range (HU)
L	0 to 4	61.2 ± 5.09	51 to 69	64.1 ± 3.83	54 to 71	100.1 ± 11.78	81 to 126	93.6 ± 10.42	78 to 118
	5 to 19	54.5 ± 6.16	44 to 69	58.5 ± 9.45	43 to 77	93.2 ± 11.78	74 to 107	88.1 ± 9.87	73 to 104
	≥ 20	45.4 ± 9.28	33 to 67	48.1 ± 9.46	35 to 65	83.2 ± 10.65	55 to 99	77.2 ± 8.39	64 to 92
S	0 to 4	50.3 ± 3.61	39 to 57	98.7 ± 12.49	73 to 140	93.7 ± 12.46	64 to 115	85.3 ± 10.54	61 to 105
	5 to 19	51.1 ± 4.255	40 to 58	101.1 ± 18.74	74 to 134	98.2 ± 9.89	79 to 113	89.4 ± 8.63	71 to 101
	≥ 20	50.4 ± 3.38	46 to 58	96.6 ± 12.97	65 to 120	98.1 ± 9.39	86 to 116	90.1 ± 7.05	81 to 102
M	0 to 4	53.8 ± 4.09	45 to 64	53.9 ± 4.96	44 to 67	55.2 ± 5.31	46 to 71	55.3 ± 5.04	45 to 67
	5 to 19	56 ± 4.36	44 to 61	56.2 ± 3.23	50 to 62	57.8 ± 3.61	50 to 63	59.5 ± 4.05	50 to 64
	≥ 20	52.3 ± 5.3	44 to 60	53.2 ± 5.31	46 to 71	55.5 ± 5.11	48 to 65	54.5 ± 5.6	47 to 65
L − *S*	0 to 4	10.9 ± 6.59	1 to 29	− 34.6 ± 1.21[b]	− 76 to − 10	6.4 ± 6.97	− 5 to 17	8.3 ± 5.29	− 1 to 19
	5 to 19	3.4 ± 5.78	− 5 to 17	− 42.6 ± 1.94[b]	− 73 to − 2	− 5.1 ± 7.36	− 23 to 5	1.3 ± 5.97	− 10 to 8
	≥ 20	− 5 ± 8.24	− 14 to 13	− 48.4 ± 1.47[b]	− 71 to − 26	− 14.9 ± 1.19[b]	− 35 to 1	− 12.9 ± 8.31	− 25 to 6
L/*S*	0 to 4	1.23 ± 0.16	1.02 to 1.74	0.66 ± 0.78	0.46 to 0.86	1.07 ± 0.84	0.95 to 1.27	1.1 ± 0.69	0.99 to 1.28
	5 to 19	1.07 ± 0.12	0.91 to 1.33	0.59 ± 0.15	0.37 to 1.03	0.95 ± 0.76	0.78 to 1.05	0.99 ± 0.67	0.89 to 1.09
	≥ 20	0.89 ± 0.16	0.72 to 1.24	0.51 ± 0.11	0.33 to 0.71	0.85 ± 0.12	0.63 to 1.01	0.86 ± 0.89	0.73 to 1.07
L − *M*	0 to 4	7.4 ± 4.61	− 3 to 16	10.2 ± 4.95	2 to 18	44.2 ± 1.2[b]	26 to 77	38.3 ± 1.06[b]	26 to 63
	5 to 19	− 1.5 ± 4.98	− 11 to 8	2.3 ± 8.97	− 9 to 22	35.3 ± 1.16[b]	16 to 52	28.7 ± 8.9	17 to 43
	≥ 20	− 7.3 ± 9.71	− 24 to 11	− 5.4 ± 1.03[b]	− 23 to 14	27.7 ± 1.23[b]	2 to 45	22.7 ± 1.09[b]	5 to 37
L/*M*	0 to 4	1.14 ± 0.9	0.94 to 1.31	1.19 ± 0.1	1.03 to 1.36	1.8 ± 0.27	1.47 to 2.57	1.7 ± 0.22	1.44 to 2.16
	5 to 19	0.97 ± 0.84	0.82 to 1.13	1.04 ± 0.16	0.85 to 1.41	1.6 ± 0.21	1.28 to 1.96	1.48 ± 0.15	1.27 to 1.7
	≥ 20	0.87 ± 0.18	0.6 to 1.21	0.91 ± 0.18	0.62 to 1.27	1.5 ± 0.25	1.04 to 1.86	1.43 ± 0.22	1.08 to 1.8

L liver attenuation only, *S* spleen attenuation, *M* muscle attenuation, *L* − *S* difference between the hepatic and splenic attenuation, *L*/*S* liver to spleen attenuation ratio, *L* − *M*, difference between the hepatic and psoas muscle attenuation, *L*/*M* liver to psoas muscle attenuation ratio

[a]Values are mean ± standard deviation

[b]Standard deviation is greater than mean

Table 2 Results of linear regression analysis

CT types	Values	CT indices				
		L	*L* − *S*	*L*/*S*	*L* − *M*	*L*/*M*
Non-enhanced	*R*	0.675	0.684	0.670	0.660	0.661
	R^2	0.455	0.468	0.449	0.435	0.437
	SEE	7.654	7.565	7.7	7.796	7.783
Arterial phase	*R*	0.651	0.315	0.473	0.641	0.631
	R^2	0.424	0.099	0.224	0.411	0.398
	SEE	7.871	9.843	9.137	7.960	8.047
Portal inflow phase	*R*	0.552	0.739	0.735	0.520	0.467
	R^2	0.305	0.546	0.540	0.270	0.218
	SEE	8.446	6.989	7.038	8.860	9.172
Hepatic venous phase	*R*	0.580	0.821	0.816	0.555	0.490
	R^2	0.337	0.674	0.665	0.308	0.240
	SEE	8.448	5.920	6.0	8.625	9.042

All series of comparisons between pathologic fat content and CT indices are $p < 0.05$

L liver attenuation only, *L* − *S* difference between the hepatic and splenic attenuation, *L*/*S* liver to spleen attenuation ratio, *L* − *M* difference between the hepatic and psoas muscle attenuation, *L*/*M* liver to psoas muscle attenuation ratio, *R* correlation coefficient, R^2 coefficient of determination, *SEE* standard error of the estimate

if the cut-off values were chosen to yield 100% specificity (− 3.5 for *L* − *M* and 0.93 for *L*/*M*) the accuracy rates were lowered to 71%.

The cut-off values that provided a balance between sensitivity and specificity and the highest cut-off values that yielded 100% specificity for the diagnosis of presence and absence of steatosis were – 1.5 for vL − *S* and 0.98 for vL/*S* and also provided high accuracy rates (87% for each).

The cut-off values that provided a balance between sensitivity and specificity on the basis of discriminating steatosis equal to or greater than 20% and steatosis less than 20% were – 5.5 for vL − *S* and 0.94 for vL/*S* and provided the highest accuracy rates (93% and 91% respectively). When the cut-off value were chosen to yield 100% specificity (− 11 for vL − *S* and 0.87 for vL/*S*), the accuracy rates remained moderately high (87% for each).

The cut-off values and the corresponding sensitivity, specificity, positive and negative predictivity values, and accuracy rates for NECT indices and for vL − *S* and vL/*S* are summarized in Table 4 (the cut-off values of all CT indices in the diagnosis of presence and severity of steatosis are shown in online resource Table 5).

Discussion

Our study is one of the few studies that evaluate and compare the accuracy of different CT indices on both NECT and CECT scans.

Linear regression analysis confirmed very strong correlations between vL − *S*, vL/*S* and steatosis at histologic examination. *R* and R^2 values of vL − *S* and vL/*S* were higher not only than other CECT indices values but also than NECT indices values and this result is inconsistent with previous studies [17, 24, 25]. But despite these, the difference between steatosis at histologic analysis and the steatosis estimated with linear regression equations for all CT indices were too large. Therefore, we agree with previous studies [17, 25] that CT indices are not acceptable for clinical use in the quantitative estimation of steatosis.

On the other hand, the use of ROC curve analysis demonstrated that CT indices can be used to discriminate presence or absence of steatosis and to differentiate steatosis equal to or greater than 20% from steatosis less than 20%. Attenuation measurements of liver normalized with spleen on hepatic venous phase (vL − *S* and vL/*S*) had the highest predictive values in predicting the presence and severity of steatosis and the reduction in hepatic blood flow and hepatic microcirculation caused by steatosis seems to be a sensible explanation of this high accuracy. Hepatic attenuation on CECT, represents the combination of the parenchymal attenuation (attenuation on NECT) and the attenuation caused by the contrast material in blood within the sinusoids. It is known that hepatic blood flow and microcirculation are decreased in steatotic livers compared with those in normal liver. The flow in the microcirculation is more markedly reduced with severe steatosis [34–36]. Experimental studies in animal models showed an inverse correlation between the degree of fat infiltration and both total hepatic blood flow and flow in the microcirculation [37]. This reduction in hepatic blood flow and hepatic microcirculation causes an additional decrease in CT attenuation on CECT besides

Table 3 ROC curve analysis

CT types	Values	The area under the ROC curve for the diagnosis of presence and absence of steatosis					The area under the ROC curve for the diagnosis of macrovesicular steatosis of 20% or greater				
		L	*L* − *S*	*L/S*	*L* − *M*	*L/M*	*L*	*L* − *S*	*L/S*	*L* − *M*	*L/M*
Non-enhanced	AUC (SE)	0.856 (0.052)	0.866 (0.047)	0.865 (0.048)	0.914 (0.04)	0.915 (0.039)	0.874 (0.068)	0.870 (0.061)	0.876 (0.058)	0.825 (0.071)	0.819 (0.073)
	95% CI	0.755 to 0.957	0.773 to 0.958	0.772 to 0.958	0.836 to 0.992	0.836 to 0.992	0.741 to 1.008	0.750 to 0.990	0.761 to 0.990	0.685 to 0.964	0.677 to 0.961
Arterial phase	AUC (SE)	0.839 (0.056)	0.714 (0.070)	0.816 (0.058)	0.857 (0.052)	0.855 (0.051)	0.861 (0.063)	0.692 (0.079)	0.810 (0.065)	0.833 (0.062)	0.829 (0.064)
	95% CI	0.730 to 0.948	0.576 to 0.853	0.702 to 0.930	0.755 to 0.958	0.754 to 0.955	0.739 to 0.984	0.538 to 0.846	0.682 to 0.938	0.712 to 0.955	0.702 to 0.955
Portal inflow phase	AUC (SE)	0.759 (0.064)	0.912 (0.036)	0.913 (0.036)	0.757 (0.064)	0.733 (0.067)	0.819 (0.057)	0.874 (0.048)	0.873 (0.049)	0.770 (0.067)	0.705 (0.078)
	95% CI	0.634 to 0.883	0.841 to 0.983	0.842 to 0.983	0.632 to 0.882	0.601 to 0.864	0.707 to 0.956	0.779 to 0.969	0.778 to 0.969	0.640 to 0.900	0.553 to 0.857
Hepatic venous phase	AUC (SE)	0.767 (0.063)	0.933 (0.031)	0.934 (0.031)	0.794 (0.059)	0.772 (0.063)	0.852 (0.053)	0.950 (0.034)	0.947 (0.034)	0.762 (0.068)	0.687 (0.082)
	95% CI	0.643 to 0.890	0.873 to 0.994	0.874 to 0.994	0.678 to 0.910	0.648 to 0.895	0.748 to 0.956	0.884 to 1.015	0.881 to 1.013	0.628 to 0.896	0.525 to 0.848

AUC area under the curve, *SE* standard error, *CI* confidence interval, *L* liver attenuation only, *S* spleen attenuation, *M* muscle attenuation, *L* − *S* difference between the hepatic and splenic, attenuation, *L/S* liver to spleen attenuation ratio, *L* − *M* difference between the hepatic and psoas muscle attenuation, *L/M* liver to psoas muscle attenuation ratio

decreased hepatic parenchymal attenuation caused by fatty infiltration. This additional contrast may help to diagnose steatosis. In agreement with this, one study showed that the attenuation difference between the steatotic portion and the normal portion of the liver became greater after contrast enhancement compared with the non-enhanced state [38].

After considering that CECT indices may give more information regarding hepatic steatosis than NECT indices, another problematic that arises is that which CT attenuation indices and which phase of CECT is best for predicting steatosis. The performance of different CT indices on different phases of CECT in predicting steatosis were distinct in our study and the contrast material enhancement patterns of liver, spleen, and psoas muscle seem to explain these variability. The contrast enhancement of liver and spleen are stabilized at a near-steady state in late phases [28]. This results in diminished divergence between liver and spleen attenuation in late phases as seen in our study as almost equal SD of attenuation of spleen and liver on venous phase. Besides this, the SD of attenuation of liver only on late phases of CECT (P and V) was large. These may be a reasonable explanation of the high predictive value of vL/*S* and vL − *S* regarding the qualitative distinction of steatosis than other CECT indices in our study.

On the other hand, the rapid enhancement of spleen causes increased variability between spleen and liver attenuation on arterial phase [28]. The larger differences in SD of attenuation of spleen and liver on arterial phase in our study support this knowledge. Because of this we think that aL/*S* and aL − *S* is not eligible for assessing steatosis. But if the arterial phase is to be used for assessing steatosis, we propose to use attenuation of liver only (A) because the SD of attenuation of liver on NECT and arterial phase of CECT was almost equal.

These findings are in part consistent with some previous reports [26–28]. In their study, in which biopsy was used as the reference and images that were obtained 75 s after the initiation of iv contrast material administration was used in analysis, Kim et al. [26] reported that attenuation measurements of liver normalized with spleen on CECT (vL − *S* in our study) had comparable accuracy with NECT indices. In the study by Jacobs et al. [27] attenuation difference between the hepatic and splenic in late hepatic venous phases (from 80 to 128 s after initiation of the contrast administration) yielded a very high accuracy in the diagnosis of steatosis. However, the high accuracy was probably largely a result of the selection bias towards patients with high degrees of hepatic steatosis in their study. Also this study lacked pathological correlation.

But unlike these, Kodama et al. [24] reported pronounced inferiority of attenuation of liver normalized with spleen on CECT in which the images obtained with a 60-s scan delay were used as CECT images in the analyses. The lower

Table 4 Accuracy of CT attenuation indices in the qualitative diagnosis of steatosis

CT index	Accuracy of CT attenuation indices in discriminating presence and absence of steatosis						Accuracy of CT attenuation indices in discriminating 20% or greater steatosis					
	Cut-off values[a]	Sensitivity (%)	Specificity (%)	PPV (%)	NPV (%)	AR (%)	Cut-off values[b]	Sensitivity (%)	Specificity (%)	PPV (%)	NPV (%)	AR (%)
L	55.5[c]	74 (23/31)	88 (21/24)	89 (23/26)	72 (21/29)	80	50.5[c]	81 (13/16)	90 (35/39)	77 (13/17)	92 (35/38)	87
	50.5[d]	55 (17/31)	100 (24/24)	100 (17/17)	63 (24/38)	75	43.5[d]	44 (7/16)	100 (39/39)	100 (7/7)	82 (39/48)	84
L − *S*	− 4[c]	71 (22/31)	88 (21/24)	88 (22/25)	70 (21/30)	78	− 1.5[c]	75 (12/16)	92 (36/39)	80 (12/15)	90 (36/40)	87
	0[d]	52 (16/31)	100 (24/24)	100 (16/16)	62 (24/39)	73	− 5.5[d]	56 (9/16)	100 (39/39)	100 (9/9)	85 (39/46)	87
L/*S*	1.12[c]	81 (25/31)	79 (19/24)	83 (25/30)	76 (19/25)	80	0.97[c]	75 (12/16)	92 (36/39)	80 (12/15)	90 (36/40)	87
	0.99[d]	52 (16/31)	100 (24/24)	100 (16/16)	62 (24/39)	73	0.91[d]	63 (10/16)	100 (39/39)	100 (10/10)	87 (39/45)	89
L − *M*	2.5[c]	90 (28/31)	88 (21/24)	90 (28/31)	88 (21/24)	89	− 9.5[c]	63 (10/16)	97 (38/39)	91 (10/11)	86 (38/44)	87
	− 3.5[d]	48 (15/31)	100 (24/24)	100 (15/15)	60 (24/40)	71	− 11.5[d]	38 (6/16)	100 (39/39)	100 (6/6)	80 (39/49)	82
L/*M*	1.04[c]	87 (27/31)	92 (22/24)	93 (27/29)	85 (22/26)	89	0.84[c]	63 (10/16)	97 (38/39)	91 (10/11)	86 (38/44)	87
	0.93[d]	48 (15/31)	100 (24/24)	100 (15/15)	60 (24/40)	71	0.81[d]	56 (9/16)	100 (39/39)	100 (9/9)	85 (39/46)	87
vL − *S*	− 1.5[a,d]	77 (24/31)	100 (24/24)	100 (24/24)	77 (24/31)	87	− 5.5[c]	94 (15/16)	92 (36/39)	83 (15/18)	97 (36/37)	93
							− 11[d]	56 (9/16)	100 (39/39)	100 (9/9)	85 (39/46)	87
vL/*S*	0.98[c,d]	77 (24/31)	100 (24/24)	100 (24/24)	77 (24/31)	87	0.94[c]	94 (15/16)	90 (35/39)	79 (15/19)	97 (35/36)	91
							0.87[d]	56 (9/16)	100 (39/39)	100 (9/9)	85 (39/46)	87

Numbers in parentheses are raw data

PPV positive predictive value, *NPV* negative predictive value, *AR* accuracy rate, *L* liver attenuation only on non-enhanced phase, *L* − *S* difference between the hepatic and splenic attenuation on non-enhanced phase, *L*/*S* liver to spleen attenuation ratio on non-enhanced phase, *L* − *M* difference between the hepatic and psoas muscle attenuation on non-enhanced phase, *L*/*M* liver to psoas muscle attenuation ratio on non-enhanced phase, *vL* − *S* difference between the hepatic and splenic attenuation on hepatic venous phase, *vL*/*S* liver to spleen attenuation ratio on hepatic venous phase

[a]Values less than or equal to each cut-off value indicate a positive diagnosis of macrovesicular steatosis

[b]Values less than or equal to each cut-off value indicate a positive diagnosis of macrovesicular steatosis of 20% or greater

[c]Represents the cut-off value that provided a balance between sensitivity and specificity

[d]Represents the highest cut-off value that yielded 100% specificity

accuracy of CECT in Kodama's study than ours may be explained in part with shorter scan delay than ours (75–80-s delay for ours). The high iodine dose employed in our study (350 mg I/mL) than this study (320 mg I/mL) may also contribute to the high accuracy of vL − *S* in our study. Also different from our study, in the study of Kodama et al. [24], attenuation measurements were made in both left and right liver lobe and this may be another probable cause of the discrepancy. In the literature it is proposed that there is a preferential distribution of steatosis toward the right hepatic lobe in diffuse steatosis and attenuation of the right hepatic lobe was found to be lower than that of the left lobe [19].

There are a few studies investigating the accuracy of attenuation of liver normalized with muscle for assessing steatosis [30, 39]. Panicek et al. [30] suggested that muscle may be a better reference than spleen, for diagnosing steatosis on CECT. But there are marked differences in enhancement patterns of liver and muscle after contrast injection and it results in large differences in SD of attenuation of muscle and liver especially on late phases. Because of this, we think that attenuation of liver normalized with muscle on CECT is not a useful method for predicting steatosis. On the other hand, although these was a small difference, *L* − *M* and *L*/*M* had the highest AUC values for the diagnosis of presence and absence of steatosis among other NECT indices and this is somewhat surprising result. We think that muscle may be used as an internal reference on NECT.

In our study, all NECT indices showed also high diagnostic performance regarding the qualitative distinction of steatosis. But because there was no statistical difference between these attenuation indices and comparison of hepatic attenuation with an internal reference is more time consuming, we agree with Kodama et al. [24] in that measuring liver attenuation alone on NECT may be more reasonable.

We think that the real challenge is how to use these data especially with CECT. Because imaging timing influences the accuracy of CECT indices and the cut-off values for the diagnosis of steatosis as demonstrated in some other previous studies as well as our's [27, 28, 38]. Some other factors such as injection rate, contrast material amount, iodine dose, and selected tube voltage may also affect attenuation measurements and influence the cut-off value [19, 26, 28]. Intra- and interscanner variability may also has effect on hepatic attenuation measurement. Therefore the clinical usefulness of such a threshold is limited. But as long as the technical parameters are within the optimal range, these effects will be minimized [19] and we think that reproducible results can be achieved if these factors, especially imaging timing, can be standardized.

If we are to use CT for screening donor candidates, given the shortage of liver donors, using the highest cut-off value that yielded 100% specificity would be reasonable in order to minimize false-positive results. In this way the risk of excluding eligible donor candidates will be reduced. Therefore using − 11 and 0.87 as cut-off values for vL − *S* and vL/*S*, respectively, in the diagnosis of steatosis of 20% or greater would be appropriate than choosing cut-off values of − 5.5 and 0.94 for vL − *S* and vL/*S*, respectively.

Our study had limitations. First, histologic analysis on hemosiderin deposits and microvesicular steatosis was not performed and these may also affect hepatic attenuation. Second, because the actual risk of mild steatosis in LDLT donors are unclear we have the cut-off set at 20% steatosis for acceptability as a donor although 30% or higher steatosis is used in some centers as a criterion. Finally fatty changes are sometimes heterogeneously distributed with in the liver. To overcome this limitation we measured a large number of ROIs and tried to match the biopsy sites and the locations of the ROIs at CT as closely as possible.

In conclusion, attenuation measurements of liver normalized with spleen on hepatic venous phase (vL − *S*, vL/*S*), has higher predictive values not only than other CECT indices but also than NECT indices in predicting the presence and severity of steatosis and may be used in the qualitative diagnosis of steatosis with high specificities. This accuracy is particularly valuable in donor candidates because CT protocols for preoperative donor evaluation may be reviewed with the purpose of avoiding unnecessary scan phases. Even so, the absence of steatosis on CT scans does not necessarily indicate the absence of steatosis and diagnostic performance of NECT and CECT indices for clinical use in the quantitative estimation of steatosis is not acceptable. Because of this its use in the evaluation of steatosis is limited. But CT findings of steatosis may be useful in evaluating steatosis in LDLT candidates with moderate to severe steatosis who are unacceptable for liver donation. In this manner unnecessary liver biopsy may be avoided in those donor candidates. Additionally for the fact that CECT is used often without concomitant NECT, the capability of CECT for the diagnosis of hepatic steatosis is much more valuable.

Compliance with ethical standards

Conflict of interest We have no conflicts of interest to disclose.

Ethical approval This study was approved by our Institutional Review Board.

Informed consent All subjects gave written informed consent.

References

1. Schroeder T, Radtke A, Kuehl H, et al. Evaluation of living liver donors with an all-inclusive 3D multi-detector row CT protocol.

Radiology 2006; 238:900–910. https://doi.org/10.1148/radiol.2382050133.
2. Adam R, McMaster P, O'Grady JG, et al. Evolution of liver transplantation in Europe: report of the European Liver Transplant Registry. Liver Transpl 2003; 9: 1231–1243. https://doi.org/10.1016/j.lts.2003.09.018.
3. Vohra S, Goyal N, Gupta S. Preoperative CT evaluation of potential donors in living donor liver transplantation. Indian J Radiol Imaging 2014;24:350–359. https://doi.org/10.4103/0971-3026.143897.
4. Vetelainen R, van Vliet A, Gouma DJ, et al. Steatosis as a risk factor in liver surgery. Ann Surg 2007;245:20–30. https://doi.org/10.1097/01.sla.0000225113.88433.cf.
5. Trevisani F, Colantoni A, Caraceni P, et al. The use of donor fatty liver for liver transplantation: a challenge or a quagmire? J Hepatol. 1996; 22:114–121.
6. Adam R, Reynes M, Johann M, et al. The outcome of steatotic grafts in liver transplantation. Transplant Proc. 1991;23:1538–1540.
7. Behrns KE, Tsiotos GG, DeSouza NF, et al. Hepatic steatosis as a potential risk factor for major hepatic resection. J Gastrointest Surg.1998;2:292–298.
8. Nagai S, Fujimoto Y, Kamei H, Nakamura T, Kiuchi T. Mild hepatic macrovesicular steatosis may be a risk factor for hyperbilirubinaemia in living liver donors following right hepatectomy. British Journal of Surgery 2009;96: 437–444. https://doi.org/10.1002/bjs.6479.
9. Tsang LL, Chen CL, Huang TL, et al. Preoperative imaging evaluation of potential living liver donors: reasons for exclusion from donation in adult living donor liver transplantation. Transplant Proc. 2008;40:2460–2. https://doi.org/10.1016/j.transproceed.2008.07.075.
10. McCormack L, Clavien P.A. Understanding the meaning of fat in the liver. Liver Transpl. 2005; 11: 137. https://doi.org/10.1002/lt.20354.
11. Shah SA, Grant DR, Greig PD, et al. Analysis and outcomes of right lobe hepatectomy in 101 consecutive living donors. Am J Transplant 2005; 5: 2764–2769. https://doi.org/10.1111/j.1600-6143.2005.01094.x.
12. Nadalin S, Malago M, Valentin-Gamazo C, et al. Preoperative donor liver biopsy for adult living donor liver transplantation: risks and benefits. Liver Transpl 2005; 11: 980–986. https://doi.org/10.1002/lt.20462.
13. Dorwal P, Gautam D, Sharma D, et al. Donor biopsy in living donor liver transplantation: is it still relevant in a developing country? Malaysian J Pathol. 2015;37:39–43.
14. Brandhagen D, Fidler J, Rosen C. Evaluation of the donor liver for living donor liver transplantation. Liver Transpl 2003;9(10 Suppl 2):S16–S28.
15. Hwang I, Lee JM, Lee KB et al. Hepatic steatosis in living liver donor candidates: preoperative assessment by using breath-hold triple-echo MR imaging and 1H MR spectroscopy. Radiology 2014;271(3):730–738. https://doi.org/10.1148/radiol.14130863.
16. Trotter JF. Selection of donors for living donor liver transplantation. Liver Transplant 2003;9:S2–S7. https://doi.org/10.1053/jlts.2003.50221.
17. Park SH, Kim PN, Kim KW, et al. Macrovesicular hepatic steatosis in living liver donors: use of CT for quantitative and qualitative assessment. Radiology 2006;239:105–112. https://doi.org/10.1148/radiol.2391050361.
18. Chen YS, Cheng YF, De Villa VH, et al. Evaluation of living liver donors. Transplantation 2003;75 (suppl 3):S16–S19. https://doi.org/10.1097/01.TP.0000046535.49186.EB.
19. Xiaozhou Ma X, Holalkere NS, Kambadakone RA, et al. Imaging-based quantification of hepatic fat: methods and clinical applications. Radiographics. 2009;29:1253–1280. https://doi.org/10.1148/rg.295085186.
20. van Werven JR, Marsman HA, Nederveen AJ, Smits NJ, ten Kate FJ, van Gulik TM, et al. Assessment of hepatic steatosis in patients undergoing liver resection: Comparison of US, CT, T1-weighted dual-echo MR imaging, and point-resolved 1H MR spectroscopy. Radiology. 2010;256:159–68. https://doi.org/10.1148/radiol.10091790.
21. Lee SW, Park SH, Kim KW, et al. Unenhanced CT for Assessment of Macrovesicular Hepatic Steatosis in Living Liver Donors: Comparison of Visual Grading with Liver Attenuation Index. Radiology 2007;244(2):479–85. https://doi.org/10.1148/radiol.2442061177.
22. Kim SH, Lee JM, Han JK, et al. Hepatic macrosteatosis: predicting appropriateness of liver donation by using MR imaging-correlation with histopathologic findings. Radiology 2006;240(1):116–129. https://doi.org/10.1148/radiol.2393042218.
23. Russo MW, Brown RS Jr. Russo MW, Brown RS. Is the cost of adult living donor liver transplantation higher than deceased donor liver transplantation? Liver Transpl. 2004;10:467–468. https://doi.org/10.1002/lt.20102.
24. Kodama Y, Ng CS, Wu TT, et al. Comparison of CT methods for determining the fat content of the liver. AJR 2007;188:1307–12. https://doi.org/10.2214/AJR.06.0992.
25. Limanond P, Raman SS, Lassman C, et al. Macrovesicular hepatic steatosis in living related liver donors: correlation between CT and histologic findings. Radiology 2004;230: 276–280. https://doi.org/10.1148/radiol.2301021176.
26. Kim DY, Park SH, Lee SS, et al. Contrast-enhanced computed tomography for the diagnosis of fatty liver: prospective study with same-day biopsy used as the reference standard. Eur Radiol. 2010;20:359–66. https://doi.org/10.1007/s00330-009-1560-x.
27. Jacobs JE, Birnbaum BA, Shapiro MA, et al. Diagnostic criteria for fatty infiltration of the liver on contrast-enhanced helical CT. AJR 1998;171:659–64. https://doi.org/10.2214/ajr.171.3.9725292.
28. Johnston RJ, Stamm ER, Lewin JM, et al. Diagnosis of fatty infiltration of the liver on contrast enhanced CT: limitations of liver-minus-spleen attenuation difference measurements. Abdom Imaging 1998;23:409–15.
29. Lawrence DA, Oliva IB, Israel GM. Detection of hepatic steatosis on contrast-enhanced CT images: diagnostic accuracy of identification of areas of presumed focal fatty sparing. AJR Am J Roentgenol. 2012;199:44–47. https://doi.org/10.2214/AJR.11.7838.
30. Panicek DM, Giess CS, Schwartz LH. Qualitative assessment of liver for fatty infiltration on contrastenhanced CT: is muscle a better standard of reference than spleen? J Comput Assist Tomogr 1997; 21: 699–705.
31. Park YS, Park SH, Lee SS, Kim DY, Shin YM, Lee W, et al. Biopsy-proven nonsteatotic liver in adults: estimation of reference range for difference in attenuation between the liver and the spleen at nonenhanced CT. Radiology 2011;258(3):760–6. https://doi.org/10.1148/radiol.10101233.
32. Iwasaki M, Takada Y, Hayashi M, et al. Noninvasive evaluation of graft steatosis in living donor liver transplantation. Transplantation 2004;78:1501–1505.
33. Saba L, di Martino M, Bosco S, del Monte M, de Cecco CN, Lombardo V et al. MDCT classification of steatotic liver: a multicentric analysis. Eur J Gastroenterol Hepatol 2015; 27(3):290–297. https://doi.org/10.1097/MEG.0000000000000277.
34. Balci A, Karazincir S, Sumbas H, Oter Y, Egilmez E, Inandi T. Effects of diffuse fatty infiltration of the liver on portal vein flow hemodynamics. J Clin Ultrasound 2008; 36:134–140. https://doi.org/10.1002/jcu.20440.

35. Ijaz S, Yang W, Winslet MC, Seifalian AM. Impairment of hepatic microcirculation in fatty liver. Microcirculation 2003; 10 (6): 447–456. https://doi.org/10.1038/sj.mn.7800206.
36. Seifalian AM, Chidambaram V, Rolles K, Davidson BR. In vivo demonstration of impaired microcirculation in steatotic human liver grafts. Liver Transpl Surg 1998; 4:71–77.
37. Seifalian AM, Piasecki C, Agarwal A, Davidson BR. The effect of graded steatosis on flow in the hepatic parenchymal microcirculation. Transplantation 1999; 68 (6):780–784.
38. Alpern MB, Lawson TL, Foley WD, et al. Focal hepatic masses and fatty infiltration detected by enhanced dynamic CT. Radiology 1986;158:45–49. https://doi.org/10.1148/radiology.158.1.3940396.
39. Speliotes E.K, Massaro J.M, Hoffmann U, Vasan RS, Meigs JB, Sahani DV, et al. Liver fat is reproducibly measured using computed tomography in the Framingham Heart Study. J Gastroenterol Hepatol. 2008;23(6):894–899. https://doi.org/10.1111/j.1440-1746.2008.05420.x.